ACS CHEMICAL HEALTH & SAFETY

pubs.acs.org/acschas Research Article

Large-Format Additive Manufacturing and Machining Using High-Melt-Temperature Polymers. Part I: Real-Time Particulate and Gas-Phase Emissions

Aleksandr B. Stefaniak,* Lauren N. Bowers, Stephen B. Martin, Jr., Duane R. Hammond, Jason E. Ham, J. R. Wells, Alyson R. Fortner, Alycia K. Knepp, Sonette du Preez, Jack R. Pretty, Jennifer L. Roberts, Johan L. du Plessis, Austin Schmidt, Matthew G. Duling, Andrew Bader, and M. Abbas Virji

ACS Chemical Health & Safety **2021**, *28*, DOI: 10.1021/acs.chas.0c00129

Cite This: *ACS Chem. Health Saf.* 2021, 28, 190–200 Read Online

ACCESS | Metrics & More | Article Recommendations | Supporting Information

ABSTRACT: The literature on emissions during material extrusion additive manufacturing with 3-D printers is expanding; however, there is a paucity of data for large-format additive manufacturing (LFAM) machines that can extrude high-melt-temperature polymers. Emissions from two LFAM machines were monitored during extrusion of six polymers: acrylonitrile butadiene styrene (ABS), polycarbonate (PC), high-melt-temperature polysulfone (PSU), poly(ether sulfone) (PESU), polyphenylene sulfide (PPS), and Ultem (poly(ether imide)). Particle number, total volatile organic compound (TVOC), carbon monoxide (CO), and carbon dioxide (CO_2) concentrations were monitored in real-time. Particle emission rate values (no./min) were as follows: ABS (1.7×10^{11} to 7.7×10^{13}), PC (5.2×10^{11} to 3.6×10^{13}), Ultem (5.7×10^{12} to 3.1×10^{13}), PPS (4.6×10^{11} to 6.2×10^{12}), PSU (1.5×10^{12} to 3.4×10^{13}), and PESU (2.0 to 5.0×10^{13}). For print jobs where the mass of extruded polymer was known, particle yield values (g^{-1} extruded) were as follows: ABS (4.5×10^{8} to 2.9×10^{11}), PC (1.0×10^{9} to 1.7×10^{11}), PSU (5.1×10^{9} to 1.2×10^{11}), and PESU (0.8×10^{11} to 1.7×10^{11}). TVOC emission yields ranged from 0.005 mg/g extruded (PESU) to 0.7 mg/g extruded (ABS). The use of wall-mounted exhaust ventilation fans was insufficient to completely remove airborne particulate and TVOC from the print room. Real-time CO monitoring was not a useful marker of particulate and TVOC emission profiles for Ultem, PPS, or PSU. Average CO_2 and particle concentrations were moderately correlated ($r_s = 0.76$) for PC polymer. Extrusion of ABS, PC, and four high-melt-temperature polymers by LFAM machines released particulate and TVOC at levels that could warrant consideration of engineering controls. LFAM particle emission yields for some polymers were similar to those of common desktop-scale 3-D printers.

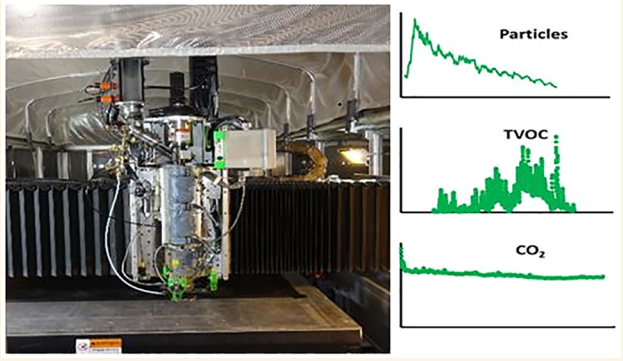

KEYWORDS: *additive manufacturing, 3-D printing, ultrafine particles, volatile organic compounds*

INTRODUCTION

Additive manufacturing (AM) refers to processes of joining materials using layer-upon-layer methodologies to build objects from a computer-aided design file.[1] One type of AM process is material extrusion, in which a solid polymer is forced through a heated nozzle, melted, and deposited in successive layers on a build platform to form an object. Variations of material extrusion AM include desktop-scale fused filament fabrication (FFF) "three-dimensional" (3-D) printers that are increasingly common in offices, libraries, schools, universities, and the home;[2] industrial-scale FFF machines used in workplaces for prototyping and production;[3] and large-format additive manufacturing (LFAM) machines used for production of tooling and other products.[4] LFAM machines differ from other types of ME technologies because they use a robot- or gantry-mounted nozzle to extrude layers of fiber-reinforced polymers at kg/h rates to build parts with dimensions that can exceed several meters in the *x*-, *y*-, and *z*-directions.[5]

Desktop-scale FFF 3-D printers are limited to extrusion of filaments conducive to the temperature capability of the extruder nozzle and/or the machine design (e.g., could lack walls to provide the necessary stable thermal environment for

Received: December 30, 2020
Published: March 25, 2021

some polymers). Polymers that are commonly extruded using these printers include acrylonitrile butadiene styrene (ABS) and polycarbonate (PC), among others, though some printers can print higher-melt-temperature polymers.[6,7] Industrial-scale FFF machines are designed to maintain a stable thermal environment and can extrude ABS and PC, as well as polymers with higher melt temperatures, such as Ultem (poly(ether imide)).[3] LFAM machines are designed to quickly extrude large amounts of the same polymers as desktop-scale and industrial-scale printers, as well as even higher-melt-temperature feedstock such as polysulfone (PSU), polyphenylene sulfide (PPS), and poly(ether sulfone) (PESU). LFAM machines use a single extruder with multiple progressively hotter zones to heat the feedstock polymer pellets until they reach a temperature just above their melting point at the nozzle, and the polymer is deposited onto a heated build platform. Given the ability to print large-scale objects, available polymer materials, reduced production costs, and shortened production times, LFAM is increasingly being used in the renewable energies, aeronautical, shipbuilding, molding, and defense industries.[5]

Numerous investigators have evaluated emissions from desktop-scale FFF 3-D printers during extrusion of ABS and PC polymers.[2,6−22] Less data are available that describes emissions from industrial-scale FFF machines, and that is limited to extrusion of ABS, PC, and Ultem polymers.[3,23] To our knowledge, only one study has evaluated emissions from an LFAM machine, and that was during extrusion of ABS.[4] Several reports have been published that described adverse toxicological and human health effects associated with emissions from extrusion of ABS using desktop-scale FFF 3-D printers.[24−28] The potential for exposure (and possible adverse effects) from other polymers (including high-melt-temperature polymers) used in LFAM is less clear.[29] Hence, the purposes of this study were to (1) evaluate real-time particle and gaseous emissions from polymers used for LFAM, (2) identify factors that influence these emissions, and (3) compare particle emissions from LFAM to the literature on desktop-scale FFF 3-D printers and industrial-scale FFF machines.

MATERIALS AND METHODS

Particulate and gaseous emissions were monitored at a workplace with two LFAM machines that produced tooling molds on a contract basis, so each print job was unique. Extrusion conditions were as follows (°C): ABS (melt = 240−270, build platform = 20−110), PC (melt = 265−305, build platform = 100−120), Ultem (melt = 385, build platform = 20−120), PPS (melt = 360, build platform = 125), PSU (melt = 350, build platform = 148), and PESU (melt = 438, build platform = 148). All polymers contained carbon fiber (CF) and/or glass fiber (GF) additive to provide structural support for large builds. Herein, the LFAM machine with a 76 m^3 internal volume is referred to as LFAM-1, and the machine with a 50 m^3 internal volume is referred to as LFAM-2. Both machines have solid metal and clear plastic sidewalls with nonsealing doors at the front and back. LFAM-1 had a custom-built loose-fitting canopy made of plastic tarpaulin fitted over a frame to enclose the build volume. LFAM-2 had a custom-built loose-fitting canopy made of reflective bubble roll insulation fitted over a frame to enclose the build volume. Both machines were in a 3000 m^3 room with two wall fans for general exhaust ventilation. The room is an open floor plan with a vaulted ceiling. One interior wall has a bay door that opens to an adjacent room that is the same dimensions and layout but houses postprocess machining tools. Air in the print room is well mixed (based on replicate air exchange measurements described below). To our knowledge, there were no zones with different air pressure that would influence accumulation of emissions in the print room.

Determination of air exchange rates inside the printer enclosures and in the printer room was made using sulfur hexafluoride (SF_6) tracer gas following ASTM standard E741-11(2017) for determining air exchange in a single zone by means of tracer gas dilution.[30] SF_6 measurements were made using photoacoustic infrared gas analyzers (Innova, Model 1412, CAI, Orange, CA). One gas analyzer was used to determine the air exchange rate inside an LFAM machine enclosure, and three analyzers at different spatial locations were used to determine the air exchange rate in the room. Table 1 summarizes the average air exchange rates determined from at least three replicate measurements of SF_6 decay. The air exchange rates were constant throughout each print job, and the fans were off or turned on prior to the start of printing.

Table 1. Average Air Exchange Rates (h^{-1}) Determined by Measurement of Sulfur Hexafluoride Decay

wall fans	LFAM-1 enclosure	LFAM-2 enclosure	room
off	13.52	8.06	0.33
1 on	14.22	8.75	2.49
2 on	14.77	8.85	5.01

Air Monitoring. Particle number concentration was enumerated in real-time before printing (background), during printing, and after printing using an isopropanol-based condensation nuclei counter (P-Trak, Model 8525, TSI Inc., Shoreview, MN) with a size range 20−1000 nm at a frequency of 1−10 s (dependent on the duration of the print job). Total volatile organic compound (TVOC) concentrations were monitored at a frequency of 1−10 s using a real-time photoionization detector (PID, Ion Science Inc., Stafford, TX) with a 10.6 eV lamp. The TVOC monitor was calibrated using isobutylene and span checked with isobutylene prior to use. Measurement results were converted to $\mu g/m^3$ as isobutylene equivalents (molecular weight = 56.11 g/mol); the stated instrument limit of detection is 1 ppb or 2.3 $\mu g/m^3$. Carbon monoxide (CO) and carbon dioxide (CO_2) concentrations were recorded using a real-time gas monitor (Model 7545, TSI Inc.) with reported measurement ranges 0−500 ppm and 0−5000 ppm, respectively; this instrument also recorded temperature and relative humidity.

Placement of Air Monitoring Equipment. The basic sampling setup consisted of a wire metal basket to hold the real-time particle, TVOC monitor, and CO/CO_2/temperature/relative humidity monitors. Within the basket, samplers were positioned such that their inlets were proximate but not adjacent to one another to prevent one sampler with a higher flow rate from drawing air away from another sampler with a lower flow rate. Figure 1 illustrates the floor plan of the printer room and the locations of sampling baskets. At LFAM-1, the inside basket was placed on the floor at the front of the machine enclosure, and the outside basket was placed at the platform that the operator normally occupied during work. At LFAM-2, the inside basket was placed on the floor at the front of the machine enclosure in a location that did not interfere with the moving extruder nozzle, and the outside basket was placed at the computer control station that the operator normally occupied during work. Baskets located inside of the enclosures were

https://doi.org/10.1021/acs.chas.0c00128
ACS Chem. Health Saf. 2021, 28, 190−200

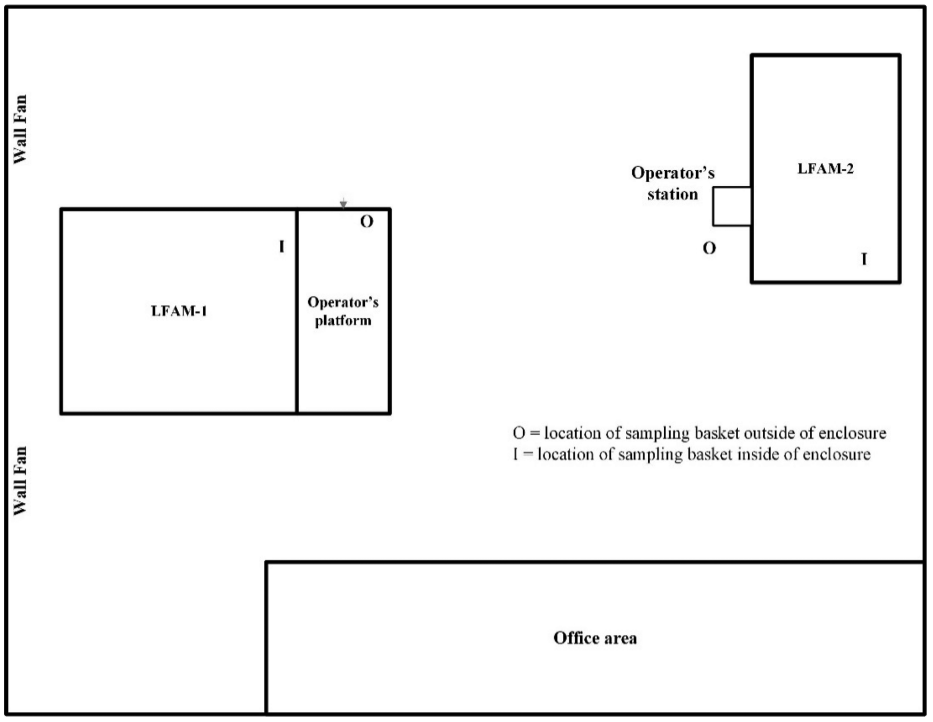

Figure 1. Printer room floor plan (not to scale) illustrating the location of LFAM machines and positioning of sampling baskets.

positioned with the sampler inlets approximately 0.3−0.5 m above the floor, and baskets located outside of the enclosures were positioned with the sampler inlets at approximately 1.2 m above the floor using a tripod (LFAM-2) or on a work bench (LFAM-2) to mimic breathing zone height (see Figure S1). All samples were collected simultaneously to one another. The location of the inside and outside samplers was the same at each LFAM during all print jobs; however, the extruder nozzle moved along a gantry during operation so its distance from the samplers varied at any given time point based on the dimensions and orientation of a print job. All prints were performed in the front half of the print bed, which minimized distance between the samplers and extruder nozzle but did not eliminate variability from the moving nozzle.

For ABS polymer, a total of six separate print jobs were monitored (designated as ABS-1−ABS-6). For PC polymer, a total of four separate print jobs were monitored (designated as PC-1−PC-4). For PPS polymer, four sequential print jobs were attempted throughout 1 day. The first two PPS polymer print attempts failed because of nozzle clogging. Inspection of the real-time instrument monitoring data for the time period of these print attempts revealed that concentration profiles for particles and gases consisted of a single large peak. Given that these two print attempts were performed sequentially, and the real-time instrument data did not distinguish between attempts, the monitoring data from the start of the first attempt to the end of the second attempt were treated as a single print for purposes of calculating emission metrics (herein grouped as job PPS-1). The latter two PPS polymer print jobs were successful (designated as PPS-2 and PPS-3). For Ultem, PSU, and PESU, a total of two print jobs were monitored for each polymer type (designated as Ultem-1, Ultem-2, PSU-1, etc.). For each print job, the LFAM was warmed up just prior to printing. The one exception was for the consecutive PPS print jobs that were grouped as PPS-1. Between print jobs for a given polymer type, the extruder nozzle was cleaned using a purge compound (ASACLEAN, Sun Plastech, Inc., Parsippany, NJ), and on three occasions, emissions were monitored during this task. Dedicated extruders were used for each polymer type. During our initial site visit (print jobs ABS-1, Ultem-1, and Ultem-2), a basket was only placed outside a machine enclosure at the operator's workstation. Thereafter, one basket was positioned inside an LFAM machine enclosure, and one basket was positioned outside of its enclosure.

Emission Rate Calculations. Average particle emission rates (ERs) were calculated using a model developed to describe emission sources in indoor environments.[31] This model has been applied to describe particle emissions from desktop-scale FFF 3-D printers and industrial-scale FFF machines in a room and workplaces:[3,32,33]

$$\mathrm{ER} = V\left[\frac{C_{\mathrm{peak}} - C_{\mathrm{background}}}{\Delta t} + \overline{\mathrm{AER} + k} \times \bar{C}_{\mathrm{avg}} - \mathrm{AER} \times C_{\mathrm{background}}\right] \quad (1)$$

Here, V = the volume of the room (or inside the LFAM machine enclosure), C_{peak} = instantaneous peak concentration of the contaminant during printing, $C_{\mathrm{background}}$ = the average background concentration of particles indoors during the few minutes preceding the start of extrusion, Δt = the time difference between C_{peak} and $C_{\mathrm{background}}$, AER = air exchange rate (h^{-1}) in the room or inside the LFAM machine enclosure as determined by measurement of SF_6 decay (Table 1), $\overline{\mathrm{AER} + k}$ = average total removal rate of particulate (AER plus k, the rate of contaminant loss due to deposition onto surfaces), and $\bar{C}_{\mathrm{avg}}$ = the average particle number concentration (cm^{-3}) of the contaminant during the entire print job. $\overline{\mathrm{AER} + k}$ is calculated as the slope of the line from a plot of time versus $\ln(C_{\mathrm{in}}/C_{\mathrm{peak}})$. C_{avg} and $C_{\mathrm{background}}$ are functions of some other factors and can vary in time.[31] Hence, to estimate the average emission rate, the equation is simplified by using average C_{avg} and $C_{\mathrm{background}}$ values instead of functions. This equation ignores the effects of particle

https://doi.org/10.1021/acs.chas.0c00128
ACS Chem. Health Saf. 2021, 28, 190−200

Table 2. Particulate Emission Characteristics by Polymer

job	LFAM[a]	location[b]	polymer[c]	additive[d] (w/w)	mass[e] (kg)	fans[f]	av (m^{-3})	C_{peak} (m^{-3})	t_{peak}[g] (min)	T[h] (min)	ER (min^{-1})	yield (g^{-1})
1[i]	2	outside	ABS	CF (20)	Unk	2	$7.7 \pm 2.7 \times 10^{10}$	1.4×10^{11}	53.2	87.0	3.0×10^{12}	N/A[j]
2	2	outside	ABS	GF (20)	118	2	$1.6 \pm 3.1 \times 10^{10}$	3.1×10^{11}	9.6	438.0	7.7×10^{13}	2.9×10^{11}
	2	inside	ABS	GF (20)	118	2	—[k]	—	—	—	—	—
3	1	outside	ABS	GF (20)	357	2	$1.2 \pm 0.4 \times 10^{10}$	3.6×10^{10}	46.9	888.0	1.1×10^{12}	2.7×10^{9}
	1	inside	ABS	GF (20)	357	2	$5.4 \pm 3.4 \times 10^{10}$	1.9×10^{11}	257.6	888.0	2.4×10^{12}	5.7×10^{10}
4	1	outside	ABS	GF (20)	Unk	0	$5.7 \pm 1.0 \times 10^{9}$	1.2×10^{10}	10.0	15.0	7.8×10^{12}	N/A
	1	inside	ABS	GF (20)	Unk	0	$1.3 \pm 0.4 \times 10^{10}$	2.3×10^{10}	0.1	15.0	1.5×10^{13}	N/A
5	1	outside	ABS	GF (20)	67	0	$3.0 \pm 1.1 \times 10^{10}$	1.3×10^{11}	174.1	207.0	3.8×10^{13}	1.2×10^{11}
	1	inside	ABS	GF (20)	67	0	$4.2 \pm 1.9 \times 10^{10}$	1.3×10^{11}	105.0	207.0	2.8×10^{11}	8.6×10^{8}
6	1	outside	ABS	CF/GF (20)	361	1	$4.0 \pm 3.0 \times 10^{10}$	2.4×10^{11}	475.0	969.0	6.0×10^{12}	1.6×10^{10}
	1	inside	ABS	CF/GF (20)	361	1	$2.3 \pm 2.8 \times 10^{10}$	1.8×10^{11}	565.3	969.0	1.7×10^{11}	4.5×10^{8}
1	1	outside	PC	CF (20)	46	0	$1.5 \pm 0.3 \times 10^{10}$	3.0×10^{10}	91.1	164.0	9.7×10^{12}	3.5×10^{10}
	1	inside	PC	CF (20)	46	0	$9.3 \pm 3.6 \times 10^{9}$	1.8×10^{10}	50.7	164.0	5.2×10^{11}	1.9×10^{9}
2	1	outside	PC	CF (20)	73	2	$3.4 \pm 1.1 \times 10^{10}$	8.7×10^{10}	43.3	121.0	1.8×10^{13}	3.0×10^{10}
	1	inside	PC	CF (20)	73	2	$1.7 \pm 0.7 \times 10^{10}$	4.6×10^{10}	71.3	121.0	7.2×10^{11}	1.2×10^{9}
3	1	outside	PC	CF (20)	Unk	2	$1.6 \pm 1.1 \times 10^{10}$	4.8×10^{10}	19.3	22.0	2.9×10^{13}	N/A
	1	inside	PC	CF (20)	Unk	2	$1.2 \pm 0.8 \times 10^{10}$	7.8×10^{10}	2.4	22.0	1.4×10^{12}	N/A
4	2	outside	PC	CF (20)	50	0	$9.1 \pm 3.8 \times 10^{10}$	2.5×10^{11}	49.0	233.0	3.6×10^{13}	1.7×10^{11}
	2	inside	PC	CF (20)	50	0	$2.2 \pm 0.8 \times 10^{10}$	4.5×10^{11}	61.1	233.0	3.4×10^{12}	1.6×10^{10}
1[i]	1	outside	Ultem	CF (20)	Unk	2	$1.7 \pm 1.3 \times 10^{10}$	1.7×10^{11}	43.3	59.0	5.7×10^{12}	N/A
2[i]	1	outside	Ultem	CF (20)	Unk	2	$2.6 \pm 1.3 \times 10^{10}$	1.1×10^{11}	17.0	29.0	3.1×10^{13}	N/A
1	1	outside	PPS	CF (50)	Unk	2	$0.8 \pm 0.5 \times 10^{10}$	4.7×10^{10}	16.4	39.0	6.2×10^{12}	N/A
	1	inside	PPS	CF (50)	Unk	2	—	—	—	—	—	—
2	1	outside	PPS	CF (50)	Unk	2	$0.9 \pm 0.5 \times 10^{10}$	4.2×10^{10}	36.7	67.0	2.3×10^{12}	N/A
	1	inside	PPS	CF (50)	Unk	2	$1.0 \pm 0.6 \times 10^{10}$	5.8×10^{10}	33.9	46.0	4.6×10^{11}	N/A
1	1	outside	PSU	CF (25)	19	2	—	—	—	—	—	—
	1	inside	PSU	CF (25)	19	2	$9.1 \pm 9.6 \times 10^{9}$	1.5×10^{11}	12.9	56.0	4.3×10^{12}	1.3×10^{10}
2	1	outside	PSU	CF (25)	207	2	$4.5 \pm 3.3 \times 10^{10}$	1.9×10^{11}	70.1	727.0	3.4×10^{13}	1.2×10^{11}
	1	inside	PSU	CF (25)	207	2	$1.7 \pm 1.0 \times 10^{11}$	5.0×10^{11}	169.5	727.0	1.5×10^{12}	5.1×10^{9}
1	1	outside	PESU	CF (25)	160	0	$1.1 \pm 0.2 \times 10^{11}$	1.9×10^{11}	252.3	56.0	2.0×10^{13}	0.8×10^{11}
	1	inside	PESU	CF (25)	160	0	—	—	—	—	—	—
2	1	outside	PESU	CF (25)	140	0	$1.0 \pm 0.2 \times 10^{11}$	1.7×10^{11}	289.5	636.0	5.0×10^{13}	1.7×10^{11}
	1	inside	PESU	CF (25)	140	0	—	—	—	636.0	—	—

[a]LFAM = large-format additive manufacturing machine 1 (76 m^3 inner volume) or 2 (50 m^3 inner volume). [b]Outside = where operator normally occupied while doing their work outside of enclosure (platform or computer station); inside = inside LFAM enclosure. [c]ABS = acrylonitrile butadiene styrene, PC = polycarbonate, PPS = polyphenylene sulfide, PSU = polysulfone, PESU = polyethersulfone. [d]CF = carbon fiber, GF = glass fiber. [e]Unk = mass extruded unknown. [f]Fans = number of wall fans operating. [g]$t_{peak} = \Delta t$ (time difference between C_{peak} and $C_{background}$) in eq 1. [h]T = total print time. [i]Only monitored outside of LFAM enclosure on initial site visit; thereafter, monitored inside and outside of LFAM enclosures. [j]N/A = not applicable. [k]— = instrument error.

dynamics (i.e., condensation, evaporation, and coagulation) as they are considered to be minor.[31] The second-by-second P-Trak measurement data were smoothed by using a 1 min moving averaging for calculations. When the mass of polymer extruded was known, emissions were expressed as particle number yield (g^{-1} of polymer extruded).

Average TVOC ERs were calculated using a model that was previously applied to gaseous emissions from a binder jetting AM machine. This model assumes that all TVOC losses were from air exchange in the workspace (i.e., no wall losses):[34]

$$\mathrm{ER} = (C_{\mathrm{TVOC},t} - C_{\mathrm{background}}) \times V \times \mathrm{AER} \quad (2)$$

Where, $C_{\mathrm{TVOC},t}$ is the instantaneous TVOC concentration at an elapsed time, t, and $C_{\mathrm{background}}$ is the average background TVOC concentration indoors during the few minutes preceding the start of extrusion.

Statistical Methods. Data plots were prepared using SigmaPlot (version 14.0, Systat Software, Inc., San Jose, CA). For all box plots, the bottom whisker is the 10th percentile, the bottom of the box the 25th percentile, the line within the box the median, the top boundary of the box the 75th percentile, and the top whisker the 90th percentile. Solid circles are outlier values.

Statistics were computed in JMP (version 13, SAS Institute Inc., Cary, NC) using a significance level of $\alpha = 0.05$ for all comparisons. All particle and TVOC emission metrics (average, peak, emission rate, emission yield) were log-transformed prior to statistical analysis. First, linear regression models were used to explore machine- (LFAM machine, print time, build platform temperature, and extruder melt temperature), feedstock- (polymer type, mass of polymer extruded, polymer additive type, and polymer additive amount), and room-related (sampling location and general exhaust ventilation) factors that could influence particle and TVOC emission metrics. The factors print time, build platform temperature, extruder melt temperature, and mass of polymer extruded were included as continuous variables and as categorical variables (three levels per factor based on the tertiles of their respective distributions) for input to models. Based on the results from the first set of models, additional linear regression models were used to identify if the significant effect of location (inside and outside of LFAM

https://doi.org/10.1021/acs.chas.0c00128
ACS Chem. Health Saf. 2021, 28, 190−200

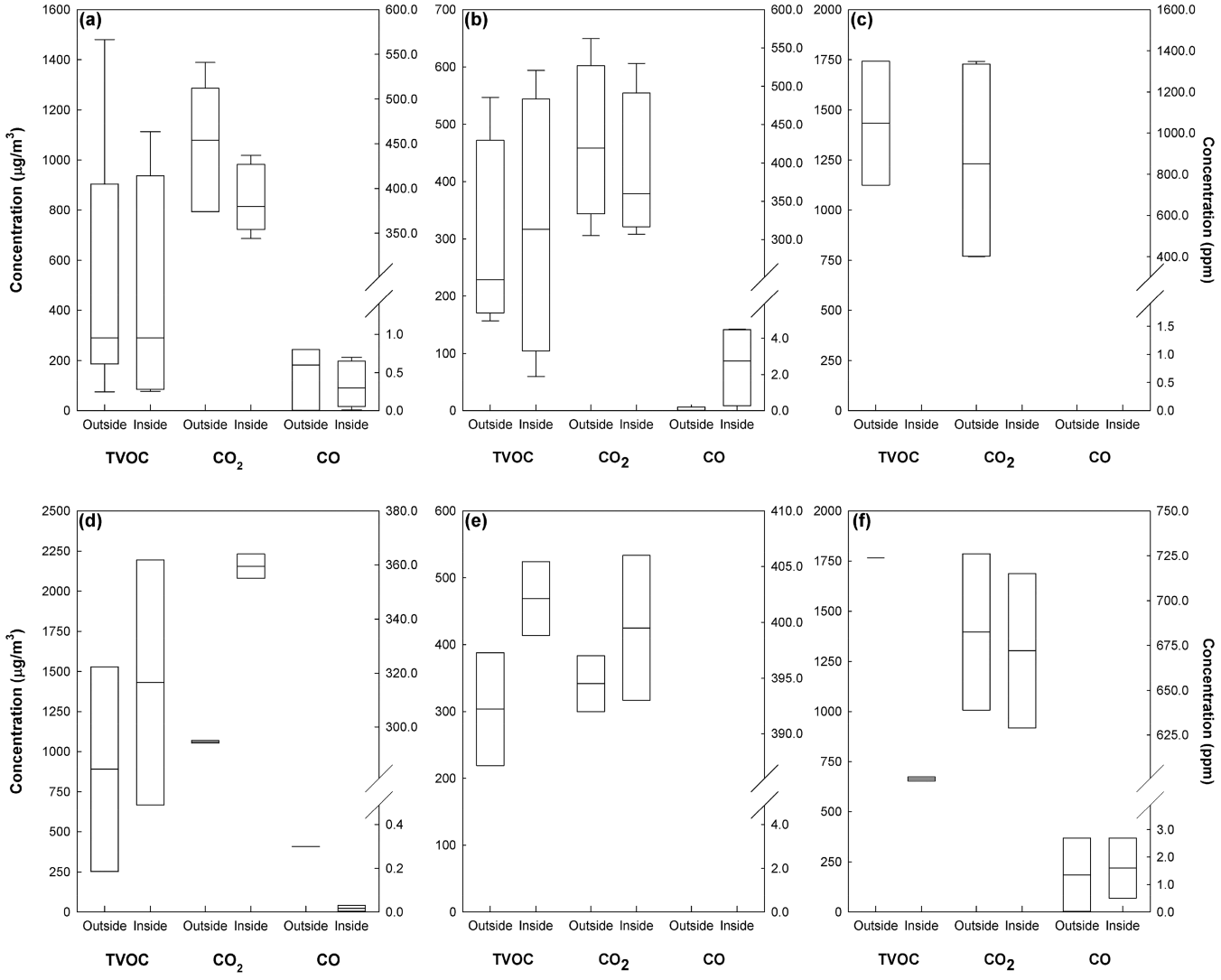

Figure 2. Box plots of average real-time TVOC (primary *y*-axis) and CO and CO_2 (secondary *y*-axis) concentrations for (a) ABS, (b) PC, (c) Ultem, (d) PPS, (e) PSU, and (f) PESU polymers.

machine enclosures) on particulate and TVOC emission rates and yields persisted after accounting for the nine factors in the stratified analysis. For TVOC data only, linear models were used to explore relationships between gas concentrations and the type and amount of additive in a polymer. Lastly, linear models were used to compare particle emission rate and yield values from these LFAM machines to published literature for desktop-scale FFF 3-D printers and industrial-scale FFF machines. Tukey's multiple comparison was used for all comparisons of means. Nonparametric Spearman's correlations were used to evaluate possible relationships between CO and CO_2 levels and particulate and TVOC levels for specific polymers that release these gases during thermal decomposition.

■ RESULTS

Emissions were monitored for 21 LFAM print jobs that encompassed six polymers and two machines on 14 different days. Print durations ranged from 15 to 969 min, and the masses of printed objects (when known) ranged from 19 to 361 kg. Print durations and extruded masses varied depending on the computer design of the part (number of slices), dimensions and complexity of the part, and the printer parameters (extrusion rate, etc.). For most print jobs, particle number and TVOC concentrations followed a temporal pattern of a rapid increase to C_{peak} early in the build cycle (i.e., t_{peak} was relatively short compared with T, the total print time) followed by a slow decay throughout the remainder of extrusion, though for some print jobs concentrations rose more slowly to reach C_{peak} and decayed thereafter (Table 2). Depending on the day, either 0, 1, or 2 wall exhaust fans were in operation.

Acrylonitrile Butadiene Styrene. As summarized in Table 2, particle ERs ranged from 1.7×10^{11} to 7.7×10^{13} min^{-1} and yields from 4.5×10^{8} to 2.9×10^{11} g^{-1} extruded. Figure 2a is box plots of the real-time TVOC and gas monitoring results (values by print job are given in Table S1). During extrusion of ABS polymer, the average TVOC ER outside the LFAM enclosures for all print jobs was 61 ± 110 mg/min (range: 1.7−284 mg/min), and inside the enclosures it was 148 ± 326 mg/min (range: 1.3−732 mg/min). TVOC yield values were 0.2 ± 0.4 mg/g extruded (range: 0.005−0.8 mg/g extruded) and 0.7 ± 1.4 mg/g extruded (range: 0.004−2.7 mg/g extruded), for the inside and outside locations, respectively. Peak CO levels did not exceed 1.5 ppm, and peak CO_2 levels ranged from 313 to 2795 ppm at all locations.

https://doi.org/10.1021/acs.chas.0c00128
ACS Chem. Health Saf. 2021, 28, 190−200

Polycarbonate. Calculated particle ERs spanned 3 orders of magnitude (10^{11}−10^{13} min^{-1}). Yield values ranged from 1.0×10^9 to 1.7×10^{11} g^{-1} extruded (see Table 2). Results of the real-time TVOC and gas monitoring during extrusion of PC polymer are summarized in Figure 2b, and details by print job are in Table S2. Average TVOC ER values for all print jobs were 3.3 ± 2.1 mg/min (range: 1.7−6.3 mg/min) and 2.0 ± 1.5 mg/min (range: 0.5−4.0 mg/min), outside and inside the LFAM enclosures, respectively. Corresponding emission yield values outside and inside the enclosures were 0.008 ± 0.005 mg/g extruded (range: 0.003−0.012 mg/g extruded) and 0.008 ± 0.006 mg/g extruded (range: 0.001−0.014 mg/g extruded). CO concentrations inside the LFAM enclosure reached almost 5 ppm. CO_2 levels were relatively constant and did not exhibit the same temporal patterns as particle concentration measurements (see Figure S2 as a representative example for particle number concentration and CO_2 levels observed for some PC print jobs).

Ultem. For extrusion of Ultem polymer, calculated ERs ranged from 5.7×10^{12} to 3.1×10^{13} min^{-1} (Table 2). The real-time TVOC and gas sampling results are given in Figure 2c (detailed results by print job given in Table S3). TVOC concentrations ranged from ∼600 to 9000 $\mu g/m^3$ across print jobs. Outside of the LFAM enclosure, the average TVOC ER for all print jobs was 110 ± 1 mg/min (range: 109−110 mg/min); TVOC levels were not monitored inside the machine enclosure. No CO was detected, though CO_2 was present between 1260 and 3600 ppm. Average CO_2 levels were similar between print jobs, and concentrations did not exhibit the same temporal concentration pattern as observed for real-time particle number or TVOC concentrations (plots not shown).

Polyphenylene Sulfide. For the failed print attempts during which the extruder nozzle clogged (grouped as job PPS-1), the real-time particle concentration profile consisted of a single large peak; during this period, the average and peak particle number concentrations and ER at the operator's platform were 1.6 ± 0.8 × 10^{10} m^{-3}, 9.0 × 10^{10} m^{-3}, and 1.1 × 10^{14} min^{-1}, respectively. Table 2 summarizes the results of the two successful prints (jobs PPS-2 and PPS-3). Particle ERs ranged from 4.6×10^{11} to 6.2×10^{12} min^{-1}. TVOC and gas monitoring results are summarized in Figure 2d. Real-time TVOC and gas monitoring results for PPS extrusion by print job are summarized in Table S4. Average TVOC ER values for all print jobs were 41 ± 18 mg/min (range: 24−60 mg/min) and 14 ± 4 mg/min (range: 10−17 mg/min) for the outside and inside locations, respectively. CO concentrations did not exceed 1 ppm. Average CO_2 concentrations ranged from approximately 300 to 350 ppm and were similar to the background. Neither CO nor CO_2 concentrations exhibited the same temporal concentration patterns as particle number or TVOC concentrations (plots not shown).

Polysulfone. During extrusion of PSU, particle ERs were from 1.5×10^{12} to 3.4×10^{13} min^{-1} and yields ranged from 5.1×10^9 to 1.2×10^{11} g^{-1} extruded (see Table 2). Results of the real-time TVOC and gas monitoring during extrusion of PSU polymer are summarized in Figure 2e, and detailed results by print job are given in Table S5. For all print jobs, the average TVOC ER outside the LFAM enclosure was 41 ± 10 mg/min (range: 34−49 mg/min), but inside the enclosure it was 4 ± 2 mg/min (range: 2−5 mg/min). The average TVOC yield values were 0.13 ± 0.02 mg/g extruded (range: 0.12−0.15 mg/g extruded) and 0.012 ± 0.009 mg/g extruded (range: 0.005−0.018 mg/g extruded), outside and inside. Almost no CO was measured during either PSU print job. Average CO_2 concentrations were approximately 400 ppm and showed little increase above background or variability during a single print job. Neither CO nor CO_2 levels exhibited the same temporal concentration patterns as particle number or TVOC concentrations (plots not shown).

Polyethersulfone. For PESU polymer, particle ERs ranged from 2.0×10^{13} to 5.0×10^{13} min^{-1} (see Table 2). Yield values were from 0.8×10^{11} to 1.7×10^{11} g^{-1} extruded. Figure 2f summarizes the real-time TVOC and gas monitoring results during extrusion of PESU polymer (detailed results by print job are summarized in Table S6). For PESU-1, the TVOC ER value outside the LFAM enclosure was 11 mg/min (a meaningful ER value could not be calculated from the monitoring data collected inside the enclosure). For PESU-2, the TVOC ER value inside the LFAM enclosure was 1 mg/min (an instrument failure precluded calculation of an ER for the outside location on that day). Average CO levels were higher during print job PESU-2 compared with job PESU-1, and average CO_2 levels were similar among print jobs and sampling locations.

Extruder Nozzle Cleaning. At LFAM-1, the nozzle cleaning task (8 min duration) was monitored on one occasion at the operator's station after printing with Ultem, and the number-based ER value was 4.0×10^{13} min^{-1}. At LFAM-2, the nozzle cleaning task was monitored on two occasions, once after a PC print (14 min duration) and the other after a PSU print (9 min duration). The number-based ERs inside the LFAM-2 enclosure were 3.1×10^{12} and 1.3×10^{12} min^{-1} for the PC and PSU prints, respectively.

Modeling of Emissions Metrics. Linear models were used to explore 10 different machine- (LFAM, print time, build platform temperature, and extruder melt temperature), feedstock- (polymer type, mass of polymer extruded, polymer additive type, and polymer additive amount), and room-related (sampling location and number of fans) factors that could influence particle emission rates and yields for samples collected inside and outside the LFAM enclosures (excluding print job PPS-1 that was influenced by nozzle clogging). For particle ER and yield, only sampling location was statistically significant. Contrary to expectation, the ER and yield values were higher outside of the LFAM machine enclosures where the machine operator worked compared with inside the enclosures ($p < 0.05$). Further statistical analyses were performed to better understand why particle ER and yields were higher outside of the LFAM machine enclosures compared with inside the enclosures. Figures S3−S11 show box plots of particle ERs and yields at the inside and outside sampling locations stratified by the remaining nine factors. After stratifying by each factor, particle ER and yield values were still higher at the outside location compared with the inside location, which indicated that none of these factors contributed to the observed differences between sampling locations.

The same linear modeling approach was used to explore factors that could influence TVOC ER and yield. TVOC ER values were significantly higher for specific levels of polymer type (Ultem > PC), extruder melt temperature (over 350 > 265−350 °C), number of wall fans in operation (two > none), and location (outside > inside enclosures). TVOC yield was not influenced by any of these factors. As with particulate, it was unclear why TVOC ER values were higher outside of the LFAM machine enclosures compared with inside the enclosures. After stratifying, it was observed that TVOC ER values were higher at the inside sampling location of LFAM-2 compared with the outside location of LFAM-2, but there was no difference by

https://doi.org/10.1021/acs.chas.0c00128
ACS Chem. Health Saf. 2021, 28, 190−200

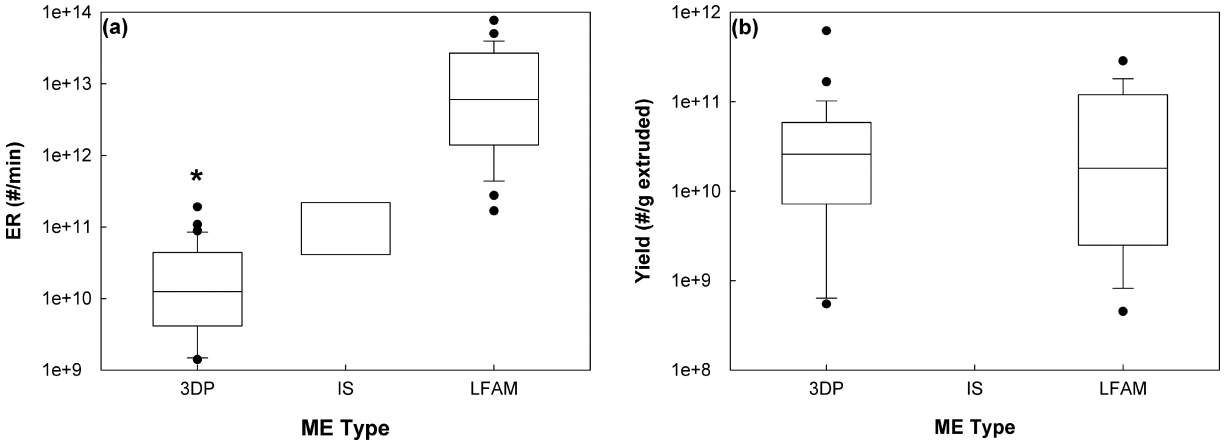

Figure 3. Box plots of particle number (a) emission rates and (b) yields by scale of machine for desktop-scale FFF 3-D printers (3DP),[6−15,17−19,33] industrial-scale FFF machines (IS),[3] and LFAM machines (current study). A label without a box plot indicates that no data are available. * = significantly different from LFAM ($p < 0.05$).

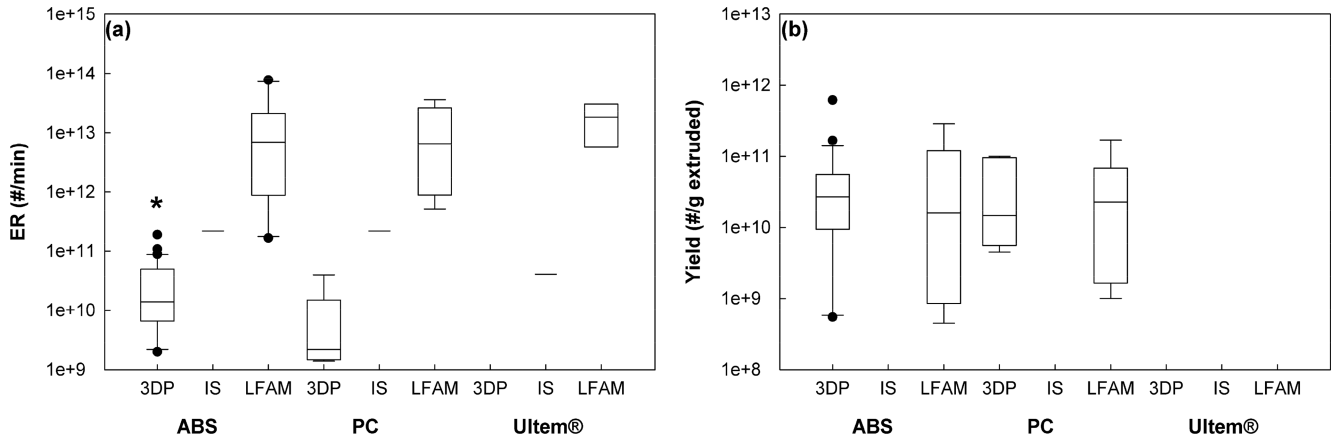

Figure 4. Box plots of particle number (a) emission rates and (b) yields by scale of machine and polymer for desktop-scale FFF 3-D printers (3DP),[6−15,17−19,33] industrial-scale FFF machines (IS),[3] and LFAM machines (current study). Dash = single data point. A label without a box plot indicates that no data are available. * = significantly different from LFAM ($p < 0.05$).

location for LFAM-1, which suggested that this factor contributed to the observed difference in ER values between sampling locations. Additionally, TVOC ER values were higher at the inside sampling location for the first tertile of print bed temperature (<120 °C) compared with the outside location (but not for the second or third tertile of print bed temperature), which suggested that this factor also contributed to the observed difference in ER values between sampling locations.

Linear models with multiple comparisons were used to evaluate relationships among average and peak TVOC levels, polymer additive type (CF or GF), and additive amount (20%, 25%, and 50%). There was no statistical difference in average TVOC concentrations between polymers with CF additive compared with GF additive or with CF additive at any amount. Peak TVOC concentrations did not differ between polymers with CF and GF additive, though peak TVOC levels were significantly higher for polymers with 50% CF additive compared with 20% CF additive ($p < 0.05$).

Relationships of CO and CO_2 with Particulate and TVOC. Comparison of CO and CO_2 data plots with field sampling notes did not reveal any influences on concentrations from workers. All average CO concentrations (Tables S1−S6) during printing were below the NIOSH recommended exposure level (REL) of 35 ppm and Occupational Safety and Health Administration (OSHA) permissible exposure limit (PEL) of 50 ppm, and average CO_2 concentrations were below the REL and PEL of 5000 ppm.[35] Nonparametric Spearman's correlations (r_s) were used to explore relationships between CO or CO_2 emissions and particulate and TVOC emissions from specific polymers. As shown in Figure S12 (CO) and Figure S13 (CO_2), correlations between gas concentrations and TVOC and particle concentrations were mostly weak. The exception was PC polymer, for which average CO_2 and TVOC levels were moderately (r_s = 0.50) and average and peak CO_2 concentrations were moderately (r_s = 0.76 and 0.67, respectively) correlated with average and peak particle number concentrations.

Scaling of Emissions among Types of Material Extrusion Machines. Figure 3 is box plots of particle number ER and yield data for desktop-scale FFF 3-D printers and industrial-scale FFF machines from the literature and LFAM machines (current study). Particle number ERs differed between LFAM machines and desktop-scale FFF 3-D printers ($p < 0.05$), though neither differed from industrial-scale FFF machines (Figure 3a). When mass of extruded polymer was accounted for, there was no statistical difference in particulate yields among scales of machines (Figure 3b). Looking at specific polymers for which data are available for all three scales of machines,

https://doi.org/10.1021/acs.chas.0c00128
ACS Chem. Health Saf. 2021, 28, 190−200

particulate ERs for ABS differed for LFAM machines compared with desktop-scale FFF 3-D printers; however, ERs for industrial-scale FFF machines did not differ from LFAM or desktop-scale FFF 3-D printers. There were no statistical differences in particle ERs for PC or Ultem by scale of machine (Figure 4a). Finally, there were no statistical differences in particulate yield values among scales of machines for ABS or PC polymers (Figure 4b). No particle emissions data are available for extrusion of PPS, PSU, and PESU polymers using desktop- and industrial-scale FFF printers.

■ DISCUSSION

To our knowledge, emissions from material extrusion AM of PPS, PSU, and PESU have not been previously reported in the literature. Herein, we reported that LFAM with these high-melt-temperature polymers, ABS, PC, and Ultem released particulate and organic gases at levels that varied by polymer.

Large-Format Additive Manufacturing/Polymer Emissions. Using a real-time particle counter (size range 20−1000 nm), we documented release of particulate during extrusion of all polymers used at this facility. Additionally, particle emission rates during a short duration nozzle cleaning task with a purge compound released particles at rates that were similar to values observed during printing with all polymers. This observation reinforces the importance of understanding exposure potential for printing as well as all other tasks in an AM process. Magalhaes et al. reviewed the available literature and concluded that a positive association exists between exposure to ambient fine particulate matter (aerodynamic diameter less <2.5 μm) and increased diastolic blood pressure, which is an indicator of increased resistance in the blood vessels (i.e., vasoconstriction).[36] Given the positive association between fine particle concentration and increased diastolic blood pressure, it is possible that inhalation of particulate released during material extrusion AM of polymers could alter cardiovascular function. Indeed, rats exposed once via nose-only inhalation for 3 h to emissions from a material extrusion-type desktop FFF 3-D printer extruding ABS developed acute hypertension.[26] In addition to submicron particles, larger particles, including CF or GF, were often present in workplace air.[29] In general, the aerodynamic diameters and aspect ratios of observed CF and GF indicate that they would have low probability for deposition in the lung alveoli.[37]

Potter et al. reported that carbon nanotubes in ABS filament generally lowered VOC emission levels from a material extrusion-type desktop FFF 3-D printer and suggested that the reduction could be due to reactivity and trapping of the organics on nanotube surfaces.[38] Wojtyla et al. indicated that addition of carbon fibers to polyethylene terephthalate filament and addition of carbon nanofibers to nylon filament significantly decreased the total amount of VOCs emitted.[39] In the current study, from linear models with multiple comparisons, average and peak TVOC concentrations did not differ significantly between polymers with CF and GF. Average TVOC concentrations did not differ by CF additive amount. Peak TVOC concentrations were higher for polymers with 25% and 50% CF additive compared with 20% CF additive. Collectively, these data indicated that micron-scale CF did not lower TVOC levels.

CO gas is released during thermal degradation of Ultem, PPS, and PSU polymers, and CO_2 gas is released during thermal degradation of these and PC polymers.[40−42] Both gases were monitored inside and outside of the LFAM machine enclosures to determine if they could be used as surrogates for particle and TVOC monitoring. The temporal concentration patterns of these gases did not follow those observed simultaneously for particulate and TVOC. Based on r_s values, CO and CO_2 levels were not useful markers of particulate or TVOC emissions for Ultem, PPS, or PSU polymers (for PPS, CO levels were negatively correlated with TVOC and particle levels, though the reason for this relationship is unknown at this time). For PC polymer, moderate correlations were observed between average and peak CO_2 and particle number, which raises the question of whether CO_2 could be used as a simple and inexpensive indicator of the magnitude (but not temporal pattern) of particle release.

Factors Influencing Emissions. Particle ER and yield values differed between the inside and outside sampling locations, but none of the machine- (LFAM machine, print time, build platform temperature, and extruder melt temperature), feedstock- (polymer type, mass of polymer extruded, polymer additive type, and polymer additive amount), and room-related (sampling location and general exhaust ventilation) factors explored in models were significant in linear models. Other factors, such as the placement of the sampling baskets inside of the enclosures, which were positioned at a height of less than 0.5 m above the floor (to not interfere with the moving extruder nozzle), could have affected emissions monitoring data. Importantly, linear models revealed that, for particulate emissions, the use of wall fans in the print room did not influence emission levels. The walls of the LFAM machines are not sealed so that the custom-built canopies positioned over the machines can be removed to access printed parts. Within the enclosure, the movement of the extruder nozzle during printing and rising warm air currents from the heated build platform resulted in air exchange rates that were a factor of 1.8−41 times higher than in the room (Table 1). One hypothesis is that particles that formed inside the machine enclosures during printing were quickly transported along rising air currents and migrated through gaps in the machine walls, doors, and canopy and into the print bay at an air exchange rate faster than removal from the room, which resulted in a net accumulation in the printer room. As noted, if the sampling basket inside the enclosure was not in the path of the rising air currents, the real-time monitor could have undercounted particle concentration. Another hypothesis is that the rate of particle formation outside of the enclosures was similar to, or exceeded, the rate of removal by the exhaust fans. It is postulated that semivolatile organic compounds that are released from thermal degradation of feedstock polymer during material extrusion AM condense to form primary particles, which in turn, grow in size because of condensation of VOCs and form agglomerates.[8,17] If some fraction of released organic gases carried by warm air currents did not condense to form particulate until reaching the relatively cooler air outside of the LFAM enclosures, the rate of particle formation could have exceeded the air removal capacity of the wall exhaust fans, though overall TVOC ER values were significantly lower inside of the enclosures compared with outside. As the extruder nozzle traveled along its build path, depending on the dimensions of the part and the build orientation, it was sometimes near the machine wall, and at other times it was near the center of the build platform. When near the walls, the distance gases and particles would travel along air currents to escape via gaps in the enclosure was less than when the nozzle was at the center of the build platform. Real-time particle sizing instruments were not available to compare

https://doi.org/10.1021/acs.chas.0c00128
ACS Chem. Health Saf. 2021, 28, 190−200

size distributions inside and outside of the enclosures but would have helped to better understand semivolatile gas condensation and particle agglomeration kinetics.

After stratifying each factor, it was observed that LFAM and print bed temperature contributed to differences in ER values between outside and inside sampling locations. Specifically, TVOC ER values were higher at the inside sampling location of LFAM-2 compared with the outside location of LFAM-2 and for the lowest tertile of print bed temperature compared with the second and third tertiles. Given the relatively lower air exchange rates inside LFAM-2 compared with LFAM-1 (see Table 1) and less thermal current emanating from the print bed at lower temperatures, we hypothesize that more organic gases accumulated within the smaller inner build volume of LFAM-2 compared with LFAM-1 (50 versus 76 m^3), which contributed to the higher observed TVOC ER values at the inside location for this machine.

Independent of whether particulate formed inside and/or outside of the machine enclosures, the source of organic gases was the extruder nozzle where polymer is heated to its melting point. If a reduction in particle and gas emissions is deemed necessary, considerations should be given to local exhaust ventilation of the machine enclosure or at the extruder nozzle to remove organic gases at the point of release rather than general room ventilation.

Comparison of Material Extrusion Type Printer Particulate Emissions. The scale of material extrusion AM machines spans from desktop-scale FFF 3-D printers to industrial-scale FFF machines to LFAM machines. Differentiating factors among these variations of material extrusion AM include (but are not limited to) the scale of the machines (build volumes), extrusion rates, and types of polymers. Desktop-scale FFF 3-D printers have the smallest build volume (e.g., 0.01−0.02 m^3) and typically extrude polymer filament at a rate of a few grams per hour (depending on printing parameters). Industrial-scale FFF machines have relatively larger build volumes (e.g., 0.03−0.06 m^3), an enclosed design, and extrude polymer filament at a rate of 10s of grams of polymer per hour. LFAM machines have the largest build volumes (e.g., >50 m^3) among material extrusion AM machines and extrude polymer pellets at a rate of several kilograms per hour. Given differences in extrusion rates and print job duration among studies in the literature, it is not appropriate to intercompare data based on emission rates. Rather, emissions data should be expressed as yield to permit a more direct comparison of results that are normalized to mass of polymer extruded because it eliminates effects of differences in extrusion rates and time among studies. There was no statistical difference in particle yield values among scales of machines (Figure 3b) or among ABS or PC polymers by scale of machines (Figure 4b). Other factors such as part design (raft, infill pattern, and density, etc.) also contribute to variability in emissions among scales of machines.[22,43] Recognizing that not all possible factors that could influence emissions were accounted for in our comparisons of scales of material extrusion machines, overall, the data indicated that emissions control is an important consideration for material extrusion AM processes in general and not just an occupational issue for larger-scale machines.

Summary. Prior studies have reported characteristics of emissions from material extrusion AM processes with common polymers such as ABS and to a lesser degree PC; however, there is little data on high-melt-temperature polymers such as PSU, PPS, Ultem, and PESU. Results presented herein indicated that these high-melt polymers, when extruded on LFAM machines, emitted particles and gases and that characteristics varied by polymer type. None of the factors included in linear regression models explained why particle emission rates were higher in the workplace compared with inside the LFAM enclosures. TVOC emission rates were also higher outside the LFAM enclosures compared with inside the LFAM enclosures. Two factors (machine) and print bed temperature (<120 °C) contributed to the observed difference in TVOC ER values at LFAM-2 between sampling locations. These findings suggest that TVOC emissions could be modulated by the choice of machine and print bed temperature; however, in practice it is impractical not to print with LFAM-2 or possible to raise the print bed temperature for some polymers because it will cause warping of the part. Hence, to reduce emissions and exposures, local exhaust ventilation should be implemented rather than general room ventilation. Based on particle yield data, which accounted for the mass of extruded polymer, there was no statistical difference in the rate of particle release among LFAM machines and literature values for desktop-scale FFF 3-D printers and industrial scale FFF machines. Custom-built canopies fitted over the LFAM machines failed to contain emissions inside the machine enclosures, and wall-mounted general exhaust fans in the printer room were insufficient to remove contaminants from workplace air. Nine factors were modeled to understand why particle and TVOC concentrations were higher outside of the LFAM enclosures compared with inside the enclosures, but the exact reason remains unknown. The mixed composition of emissions, which included particulate and gases, could present challenges for engineering controls as their removal efficiency depends on different physical and chemical processes (e.g., filtration for particles and adsorption for gases).[33] Based on the data collected, future work will focus on whether exhaust ventilation for the LFAM enclosure or local exhaust ventilation at the extruder nozzle provides a better reduction in emissions.

■ ASSOCIATED CONTENT

Supporting Information

The Supporting Information is available free of charge at https://pubs.acs.org/doi/10.1021/acs.chas.0c00128.

Summary statistics for gas concentrations by print job, photographs of sampler positioning outside of the LFAM machines, a plot of particle and CO_2 concentrations, and box plots of particle emission metrics by machine-, feedstock-, and room-related factors (PDF)

■ AUTHOR INFORMATION

Corresponding Author

Aleksandr B. Stefaniak − *National Institute for Occupational Safety and Health, Morgantown, West Virginia 26505, United States;* orcid.org/0000-0003-3914-1460; Phone: +1-304-285-6302; Email: AStefaniak@cdc.gov

Authors

Lauren N. Bowers − *National Institute for Occupational Safety and Health, Morgantown, West Virginia 26505, United States*

Stephen B. Martin, Jr. − *National Institute for Occupational Safety and Health, Morgantown, West Virginia 26505, United States*

Duane R. Hammond − *National Institute for Occupational Safety and Health, Cincinnati, Ohio 45213, United States*

Jason E. Ham − *National Institute for Occupational Safety and Health, Morgantown, West Virginia 26505, United States;* orcid.org/0000-0001-7707-1550
J. R. Wells − *National Institute for Occupational Safety and Health, Morgantown, West Virginia 26505, United States;* orcid.org/0000-0002-3472-0028
Alyson R. Fortner − *National Institute for Occupational Safety and Health, Morgantown, West Virginia 26505, United States*
Alycia K. Knepp − *National Institute for Occupational Safety and Health, Morgantown, West Virginia 26505, United States*
Sonette du Preez − *North-West University, Occupational Hygiene and Health Research Initiative, Potchefstroom 2520, South Africa*
Jack R. Pretty − *National Institute for Occupational Safety and Health, Cincinnati, Ohio 45213, United States*
Jennifer L. Roberts − *National Institute for Occupational Safety and Health, Cincinnati, Ohio 45213, United States*
Johan L. du Plessis − *North-West University, Occupational Hygiene and Health Research Initiative, Potchefstroom 2520, South Africa*
Austin Schmidt − *Additive Engineering Solutions, Akron, Ohio 44305, United States*
Matthew G. Duling − *National Institute for Occupational Safety and Health, Morgantown, West Virginia 26505, United States*
Andrew Bader − *Additive Engineering Solutions, Akron, Ohio 44305, United States*
M. Abbas Virji − *National Institute for Occupational Safety and Health, Morgantown, West Virginia 26505, United States*

Complete contact information is available at: https://pubs.acs.org/10.1021/acs.chas.0c00128

Notes

The authors declare no competing financial interest.

■ ACKNOWLEDGMENTS

The authors thank Dr. Stefan Linde (North West University) and Dr. Gary Roth (NIOSH) for critical review of this manuscript prior to submission to the journal. We also thank the company where these measurements were performed for access to their facility. The findings and conclusions in this report are those of the authors and do not necessarily represent the official position of the National Institute for Occupational Safety and Health, Centers for Disease Control and Prevention. This work was supported by NIOSH intramural research funds. The South African Department of Science and Innovation through the Competitive Programme in Additive Manufacturing funded the research visit of J.L.d.P. and S.d.P.

■ REFERENCES

(1) *Additive manufacturing—general principles—terminology*; ISO/ASTM 52900; ISO: Geneva, Switzerland, 2015.
(2) Davis, A. Y.; Zhang, Q.; Wong, J. P. S.; Weber, R. J.; Black, M. S. Characterization of volatile organic compound emissions from consumer level material extrusion 3D printers. *Build Environ* **2019**, *160*, 106209.
(3) Stefaniak, A. B.; Johnson, A. R.; du Preez, S.; Hammond, D. R.; Wells, J. R.; Ham, J. E.; LeBouf, R. F.; Martin, SB J; Duling, M. G.; Bowers, L. N.; Knepp, A. K.; de Beer, D. J.; du Plessis, J. L. Insights into emissions and exposures from use of industrial-scale additive manufacturing machines. *Saf. Health Work.* **2019**, *10*, 229−36.
(4) Zontek, T. L.; Hollenbeck, S.; Jankovic, J.; Ogle, B. R. Modeling particle emissions from three-dimensional printing with acrylonitrile-butadiene-styrene polymer filament. *Environ. Sci. Technol.* **2019**, *53*, 9656−63.
(5) Moreno Nieto, D.; Molina, S. I. Large-format fused deposition additive manufacturing: A review. *Rapid Proto J.* **2019**, *26*, 793−99.
(6) Azimi, P.; Zhao, D.; Pouzet, C.; Crain, N. E.; Stephens, B. Emissions of ultrafine particles and volatile organic compounds from commercially available desktop three-dimensional printers with multiple filaments. *Environ. Sci. Technol.* **2016**, *50*, 1260−8.
(7) Floyd, E. L.; Wang, J.; Regens, J. L. Fume emissions from a low-cost 3-D printer with various filaments. *J. Occup. Environ. Hyg.* **2017**, *14*, 523−33.
(8) Ding, S.; Ng, B. F.; Shang, X.; Liu, H.; Lu, X.; Wan, M. P. The characteristics and formation mechanisms of emissions from thermal decomposition of 3D printer polymer filaments. *Sci. Total Environ.* **2019**, *692*, 984−94.
(9) Gu, J.; Wensing, M.; Uhde, E.; Salthammer, T. Characterization of particulate and gaseous pollutants emitted during operation of a desktop 3D printer. *Environ. Int.* **2019**, *123*, 476−85.
(10) Kim, Y.; Yoon, C.; Ham, S.; Park, J.; Kim, S.; Kwon, O.; Tsai, P. J. Emissions of nanoparticles and gaseous material from 3D printer operation. *Environ. Sci. Technol.* **2015**, *49*, 12044−53.
(11) Kwon, O.; Yoon, C.; Ham, S.; Park, J.; Lee, J.; Yoo, D.; Kim, Y. Characterization and control of nanoparticle emission during 3D printing. *Environ. Sci. Technol.* **2017**, *51*, 10357−68.
(12) Mendes, L.; Kangas, A.; Kukko, K.; Mølgaard, B.; Säämänen, A.; Kanerva, T.; Flores Ituarte, I.; Huhtiniemi, M.; Stockmann-Juvala, H.; Partanen, J.; Hämeri, K.; Eleftheriadis, K.; Viitanen, A. K. Characterization of emissions from a desktop 3D printer. *J. Ind. Ecol.* **2017**, *21*, S94−S106.
(13) Stefaniak, A. B.; Bowers, L. N.; Knepp, A. K.; Virji, M. A.; Birch, E. M.; Ham, J. E.; Wells, J. R.; Qi, C.; Schwegler-Berry, D.; Friend, S.; Johnson, A. R.; Martin, S. B., Jr.; Qian, Y.; LeBouf, R. F.; Birch, Q.; Hammond, D. Three-dimensional printing with nano-enabled filaments releases polymer particles containing carbon nanotubes into air. *Indoor Air* **2018**, *28*, 840−51.
(14) Steinle, P. Characterization of emissions from a desktop 3D printer and indoor air measurements in office settings. *J. Occup. Environ. Hyg.* **2016**, *13*, 121−32.
(15) Stephens, B.; Azimi, P.; El Orch, Z.; Ramos, T. Ultrafine particle emissions from desktop 3D printers. *Atmos. Environ.* **2013**, *79*, 334−39.
(16) Vaisanen, A. J. K.; Hyttinen, M.; Ylonen, S.; Alonen, L. Occupational exposure to gaseous and particulate contaminants originating from additive manufacturing of liquid, powdered and filament plastic materials and related post-processes. *J. Occup. Environ. Hyg.* **2019**, *16*, 258−71.
(17) Vance, M. E.; Pegues, V.; Van Montfrans, S.; Leng, W.; Marr, L. C. Aerosol emissions from fuse-deposition modeling 3D printers in a chamber and in real indoor environments. *Environ. Sci. Technol.* **2017**, *51*, 9516−23.
(18) Yi, J.; LeBouf, R. F.; Duling, M. G.; Nurkiewicz, T. R.; Chen, B. T.; Schwegler-Berry, D.; Virji, M. A.; Stefaniak, A. B. Emission of particulate matter from a desktop three-dimensional (3-D) printer. *J. Toxicol. Environ. Health, Part A* **2016**, *79*, 453−65.
(19) Zhang, Q.; Wong, J. P. S.; Davis, A. Y.; Black, M. S.; Weber, R. J. Characterization of particle emissions from consumer fused deposition modeling 3D printers. *Aerosol Sci. Technol.* **2017**, *51*, 1275−86.
(20) Zhou, Y.; Kong, X.; Chen, A.; Cao, S. Investigation of ultrafine particle emissions of desktop 3D printers in the clean room. *Procedia Eng.* **2015**, *121*, 506−12.
(21) Zontek, T. L.; Ogle, B. R.; Jankovic, J. T.; Hollenbeck, S. M. An exposure assessment of desktop 3D printing. *J. Chem. Health Saf.* **2017**, *24*, 15−25.
(22) Cheng, Y. L.; Zhang, L. C.; Chen, F.; Tseng, Y. H. Particle emissions of material-extrusion-type desktop 3D printing: The effects of infill. *Int. J. Precis Eng. Manuf - Green Tech* **2018**, *5*, 487−97.
(23) du Preez, S.; Johnson, A. R.; LeBouf, R. F.; Linde, S. J. L.; Stefaniak, A. B.; Du Plessis, J. Exposures during industrial 3-D printing and post-processing tasks. *Rapid Proto J.* **2018**, *24*, 865−71.

(24) Chan, F. L.; House, R.; Kudla, I.; Lipszyc, J. C.; Rajaram, N.; Tarlo, S. M. Health survey of employees regularly using 3D printers. *Occup Med. (Lond)* **2018**, *68*, 211−14.
(25) House, R.; Rajaram, N.; Tarlo, S. M. Case report of asthma associated with 3D printing. *Occup Med. (Lond)* **2017**, *67*, 652−54.
(26) Stefaniak, A. B.; LeBouf, R. F.; Duling, M. G.; Yi, J.; Abukabda, A. B.; McBride, C. R.; Nurkiewicz, T. R. Inhalation exposure to three-dimensional printer emissions stimulates acute hypertension and microvascular dysfunction. *Toxicol. Appl. Pharmacol.* **2017**, *335*, 1−5.
(27) Zhang, Q.; Pardo, M.; Rudich, Y.; Kaplan-Ashiri, I.; Wong, J. P. S.; Davis, A. Y.; Black, M. S.; Weber, R. J. Chemical composition and toxicity of particles emitted from a consumer-level 3d printer using various materials. *Environ. Sci. Technol.* **2019**, *53*, 12054−61.
(28) Farcas, M. T.; Stefaniak, A. B.; Knepp, A. K.; Bowers, L.; Mandler, W. K.; Kashon, M.; Jackson, S. R.; Stueckle, T. A.; Sisler, J. D.; Friend, S. A.; Qi, C.; Hammond, D. R.; Thomas, T. A.; Matheson, J.; Castranova, V.; Qian, Y. Acrylonitrile butadiene styrene (abs) and polycarbonate (pc) filaments three-dimensional (3-d) printer emissions-induced cell toxicity. *Toxicol. Lett.* **2019**, *317*, 1−12.
(29) Stefaniak, A.; Bowers, L.; Martin, J. S.; Hammond, D.; Ham, J.; Wells, J.; Fortner, A.; Knepp, A.; du Preez, S.; Pretty, J. R.; Roberts, J. L.; du Plessis, J.; Duling, M. G.; Virji, M. A. Large-Format Additive Manufacturing and Machining Using High-Melt-Temperature Polymers. Part II: Characterization of Particulate and Gases. *ACS Chem. Health Safety* **2021**, in press. DOI: 10.1021/acs.chas.0c00129
(30) *Standard test method for determining air change in a single zone by means of a tracer gas dilution*; ASTM E741-11; ASTM: West Conshohocken, PA, 2017.
(31) He, C.; Morawska, L.; Hitchins, J.; Gilbert, D. Contribution from indoor sources to particle number and mass concentrations in residential houses. *Atmos. Environ.* **2004**, *38*, 3405−15.
(32) Stabile, L.; Scungio, M.; Buonanno, G.; Arpino, F.; Ficco, G. Airborne particle emission of a commercial 3D printer: The effect of filament material and printing temperature. *Indoor Air* **2017**, *27*, 398−408.
(33) Stefaniak, A. B.; Johnson, A. R.; du Preez, S.; Hammond, D. R.; Wells, J. R.; Ham, J. E.; LeBouf, R. F.; Menchaca, K. W.; Martin, SB J; Duling, M. G.; Bowers, L. N.; Knepp, A. K.; Su, F. C.; de Beer, D. J.; du Plessis, J. L. Evaluation of emissions and exposures at workplaces using desktop 3-dimensional printers. *J. Chem. Health Saf.* **2019**, *26*, 19−30.
(34) Afshar-Mohajer, N.; Wu, C. Y.; Ladun, T.; Rajon, D. A.; Huang, Y. Characterization of particulate matters and total voc emissions from a binder jetting 3D printer. *Build Environ* **2015**, *93*, 293−301.
(35) NIOSH. *Pocket Guide to Chemical Hazards*, 2018. http://www.cdc.gov/niosh/npg/default.html (accessed January 29, 2021).
(36) Magalhaes, S.; Baumgartner, J.; Weichenthal, S. Impacts of exposure to black carbon, elemental carbon, and ultrafine particles from indoor and outdoor sources on blood pressure in adults: A review of epidemiological evidence. *Environ. Res.* **2018**, *161*, 345−53.
(37) Oberdorster, G. Toxicokinetics and effects of fibrous and nonfibrous particles. *Inhalation Toxicol.* **2002**, *14*, 29−56.
(38) Potter, P. M.; Al-Abed, S. R.; Lay, D.; Lomnicki, S. M. Voc emissions and formation mechanisms from carbon nanotube composites during 3D printing. *Environ. Sci. Technol.* **2019**, *53*, 4364−70.
(39) Wojtyła, S.; Klama, P.; Śpiewak, K.; Baran, T. 3D printer as a potential source of indoor air pollution. *Int. J. Environ. Sci. Technol.* **2020**, *17*, 207−18.
(40) Ehlers, G. F. L.; Fisch, K. R.; Powell, W. R. Thermal degradation of polymers with phenylene units in the chain. II. Sulfur-containing polyarylenes. *J. Polym. Sci., Part A-1: Polym. Chem.* **1969**, *7*, 2955−67.
(41) Huang, J.; He, C.; Li, X.; Pan, G.; Tong, H. Theoretical studies on thermal degradation reaction mechanism of model compound of bisphenol a polycarbonate. *Waste Manage.* **2018**, *71*, 181−91.
(42) Koo, J. H.; Venumbaka, S.; Cassidy, P. E.; Fitch, J. W.; Grand, A. F.; Bundick, J. Flammability studies of thermally resistant polymers using cone calorimetry. *Fire Mater.* **2000**, *24*, 209−18.
(43) Simon, T. R.; Aguilera, G. A.; Zhao, F. In *Characterization of particle emission from fuse deposition modeling printers*. Proceedings of the ASME (2017) 12th International Manufacturing Science and Engineering Conference; American Society of Mechanical Engineers: Los Angeles, CA, 2017.